STRUCTURAL CONTROL AND HEALTH MONITORING
*Struct. Control Health Monit.* 2009; **16**:657–667
Published online 31 March 2009 in Wiley InterScience
(www.interscience.wiley.com). DOI: 10.1002/stc.332

# An SMA passive device proposed within the highway bridge benchmark

F. Casciati*,†, L. Faravelli and R. Al Saleh

*Department of Structural Mechanics, University of Pavia, via Ferrata 1, 2700 Pavia, Italy*

## SUMMARY

A highway bridge benchmark problem, focused on limiting excessive displacements during a given set of seismic events, has been formulated recently. The contribution summarized in this paper presents the application of a shape memory alloy (SMA) device to this benchmark problem. The analytical model of the SMA device is incorporated in the control force equation of the sample passive device. The effects of the proposed passive device on the dynamic response of the highway bridge are studied for six ground motion excitations. The results show that the proposed passive SMA damper can aggressively limit peak bearing and displacement response quantities during strong earthquakes. However, this is achieved at the cost of an increase in peak base shear and overturning moment. Such increase can be reduced by an integrated design of the device with other components of the bridge. Copyright © 2009 John Wiley & Sons, Ltd.

KEY WORDS: passive; control; bridge; benchmark; earthquake; SMA

## INTRODUCTION

Several benchmark problems facilitating comparisons between competitive control strategies have been proposed and discussed during the last decade: low-rise buildings against seismic events [1–3] high-rise buildings against the wind action [4,5], a base-isolated building [6–9], a cable-stayed bridge under seismic and snow load combination [10–12]. More recently, a seismically excited highway bridge benchmark problem has been developed [13] to facilitate a systematic and standardized means by which competing control strategies, including devices, control algorithms and sensors, can be evaluated. The benchmark highway bridge model is based on the recently constructed 91/5 highway bridge in Southern California. This bridge is in high seismic zone and likely to be exposed to severe earthquakes.

*Correspondence to: F. Casciati, Department of Structural Mechanics, University of Pavia, via Ferrata 1, 2700 Pavia, Italy.
†E-mail: fabio@dipmec.unipv.it

Contract/grant sponsor: Athenaeum Research Fund of the University of Pavia

*Received 8 April 2008*
*Revised 19 January 2009*
*Accepted 23 January 2009*

The highway bridge benchmark problem consists of two phases. Phase I problem studies the case when the deck is fixed to the outriggers in the center of the bridge. In Phase II benchmark problem, the deck is isolated from the outriggers by lead–rubber bearings. In this paper, the Phase II highway benchmark bridge model is used to investigate the effects achieved by adopting a shape memory alloy (SMA) passive device.

## THE CASE STUDY

The bridge under investigation consists of a pre-stressed concrete box-girder deck, supported by abutments at each side, and by two columns located under the mid-span of the deck (Figure 1). The resulting finite element model for the structural system has 430 degrees of freedom. It represents the full evaluation model; a reduced-order model is only used for the controller design.

The reduced-order model is derived from the full order evaluation model. It was obtained by capturing the dynamics of the full order model accurately. The reduced-order model is represented by the following state-space system of equations:

$$\dot{x} = Ax + Bf + E\ddot{u}_g \tag{1}$$

$$y_z = C^z x + D^z f + F^z \ddot{u}_g \tag{2}$$

$$y_m = C^m x + D^m f + F^m \ddot{u}_g \tag{3}$$

In the above equations, $x$ refers to the states of the system, while $A$, $B$ and $E$ are the state matrices of the system, $\ddot{u}_g$ is the ground acceleration vector in the two horizontal directions and $f$ is the vector of the control forces. The vectors $y_z$ and $y_m$ represent the regulated and measured outputs, as given by Equations (2) and (3), respectively. The matrices $C$, $D$ and $F$ are mapping matrices of appropriate dimensions. The benchmark problem has a prescribed set of six two-components horizontal acceleration time histories (Table I) to be used as ground motion excitation: Each of these ground motions is applied synchronously to the six supports.

The Phase II benchmark bridge is isolated by lead–rubber bearings both at abutments and at the outrigger, as shown in Figure 2, and two dampers (one in each of the two horizontal directions) can be added as passive structural control tools. The benchmark model utilizes LRB bearings, which have nonlinear behavior in two directions. The benchmark problem package consists of detailed modeling of

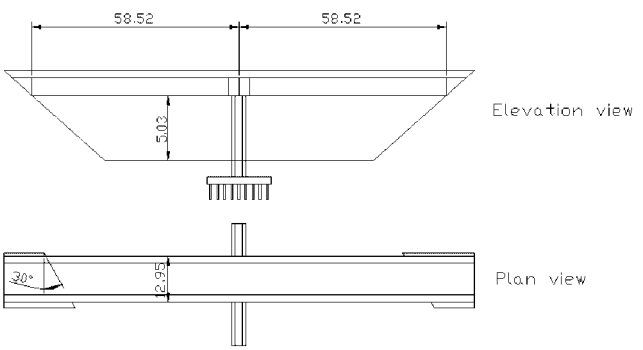


Figure 1. Elevation and plan view of the bridge.



DOI: 10.1002/stc

Table I. Properties of the earthquake acceleration records to be adopted in the benchmark problem analyses.

| Recording station | Earthquake | Magnitude | Distance to fault (km) | Peak accel. ($g$) | Peak velocity (cm/s) |
|---|---|---|---|---|---|
| North Palm Springs | 1986 N. Palm Springs | 6 | 7.3 | 0.492 | 73.3 |
| TCU084 | 1999 Chichi | 7.6 | 10.39 | 1.157 | 114.7 |
| El Centro | 1940 Imperial Valley | 7 | 8.3 | 0.313 | 29.8 |
| Rinaldi | 1994 Northridge | 6.7 | 7.1 | 0.838 | 166.1 |
| Bolu | 1999 Duzce, Turkey | 7.1 | 17.6 | 0.728 | 56.4 |
| Nishi-Akashi | 1995 Kobe | 6.9 | 11.1 | 0.509 | 37.3 |

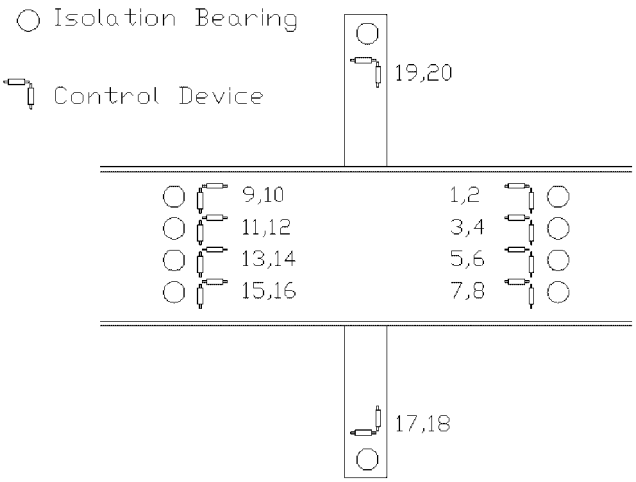


Figure 2. Locations of isolation bearings and control devices.

the bridge components, including hysteretic behavior of bearings. Additional nonlinearity can be added to incorporate the design of appropriate dampers, if desired, to achieve certain design objectives.

The benchmark bridge has nonlinear viscous dampers as sample passive devices. For the $i$th nonlinear viscous damper, the control force $f_p(i)$ is expressed as

$$f_p(i) = -c_v|v(i)|^{a_v}\text{sign}(v(i)) \tag{4}$$

where $v$ is the velocity vector across the nonlinear damper, $c_v$ is the damping coefficient and $a_v$ is the exponent to the absolute value of the velocity across the damper. The parameters of the damper in Equation (4) are assumed to be the same for all the dampers. Their values are

$$c_v = 100\,000\ \text{N/(m/s)}^{a_v}$$
$$a_v = 0.6$$

The highway bridge benchmark package also defines suitable performance evaluation criteria as a tool of comparison between different strategies [13]. The package provides sample passive, semi-active and active control strategies and evaluation criteria for those control strategies [14,15]. For the Phase II benchmark problem, Nagarajaiah *et al.* [15] presents response quantities of the bridge without any control. It is observed that the maximum bearing



DOI: 10.1002/stc

deformation varies from 10 cm during the N. Palm Spring earthquake to 55 cm during the Rinaldi record of the 1994 Northridge earthquake.

## PROPOSED PASSIVE SHAPE MEMORY ALLOY DEVICE

The first two authors introduced recently a hysteretic base isolator obtained by coupling a sliding support with inclined bars in SMA [16,17]. Figure 3(a) shows the prototype of the 3-bar SMA control device. The isolation system is designed to support a circular steel plate serving as superimposed tray, where the system to be isolated is mounted. The inclined bars are displayed in a manner to play with horizontal displacements, while the vertical load is transferred from the superimposed tray to the base by a steel cylinder. In the proposed device, the number, diameter, inclination and the geometric disposition of the SMA bars represent the design variables of the isolation system. Figure 3(b) provides a force–displacement cycle as obtained from a shaking table test by applying a sinusoidal excitation on the device. The force was estimated from the absolute acceleration measured on the upper tray; the relative displacement as the difference of the measured position of the upper tray minus that of the table.

In order to develop an analytical model of the proposed device that can show the experimental behavior in Figure 3(b), the model of nonlinear viscous damper in Equation (4) was utilized; with the parameters $c_v$ and $a_v$ as 10 000 N/(m/s) and 2, respectively. The force–displacement plot of nonlinear viscous damper with these parameters is shown in Figure 4(a). It is observed from

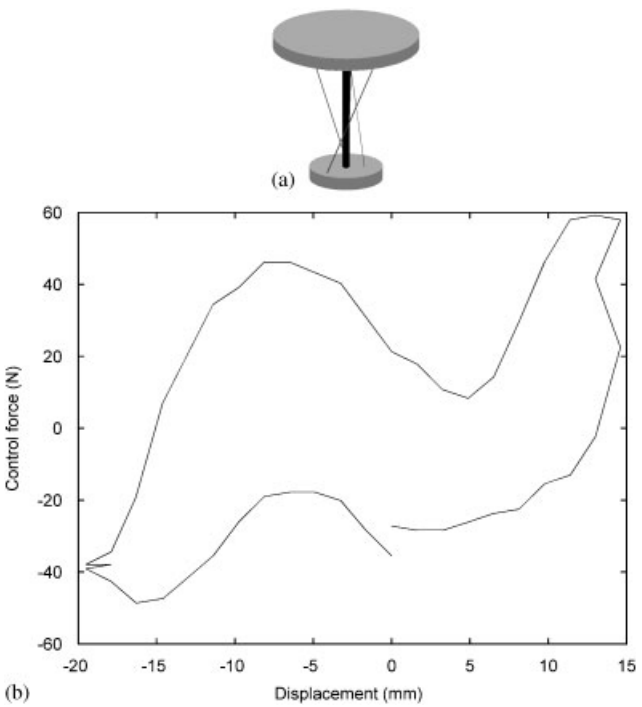


Figure 3. (a) Prototype of the SMA control device: the central shaft is supporting the vertical loads; the upper disk is sliding on it. (b) Experimental cycle of the base isolation device introduced in [16,17].



DOI: 10.1002/stc

Figure 4(a) that the hysteresis loop of the nonlinear viscous damper in Equation (4) does not have any backbone stiffness of the type observed in the experimental hysteresis loop of the proposed device in Figure 3(b). An analytical model of the proposed device is developed by the addition of an extra part (backbone stiffness) to the control force in Equation (4), which depends on the relative displacement between the bridge deck and either a side abutment or a mid-column. Hence, the resulting equation for control of the proposed device can be written as [18]

$$f_p(i) = b(-c_v \times |v(i)|^{a_v} \times \text{sign}(v(i))) + \left(k \times \left(\frac{u(i)}{u_l}\right)^{10} \times \text{sign}(u(i))\right) \tag{5}$$

where $u$ indicates the relative displacement, $u_l$ is a parameter, with the dimension of a displacement, which depends on the expected response, $k$ is a stiffness term and $b$ is a factor by

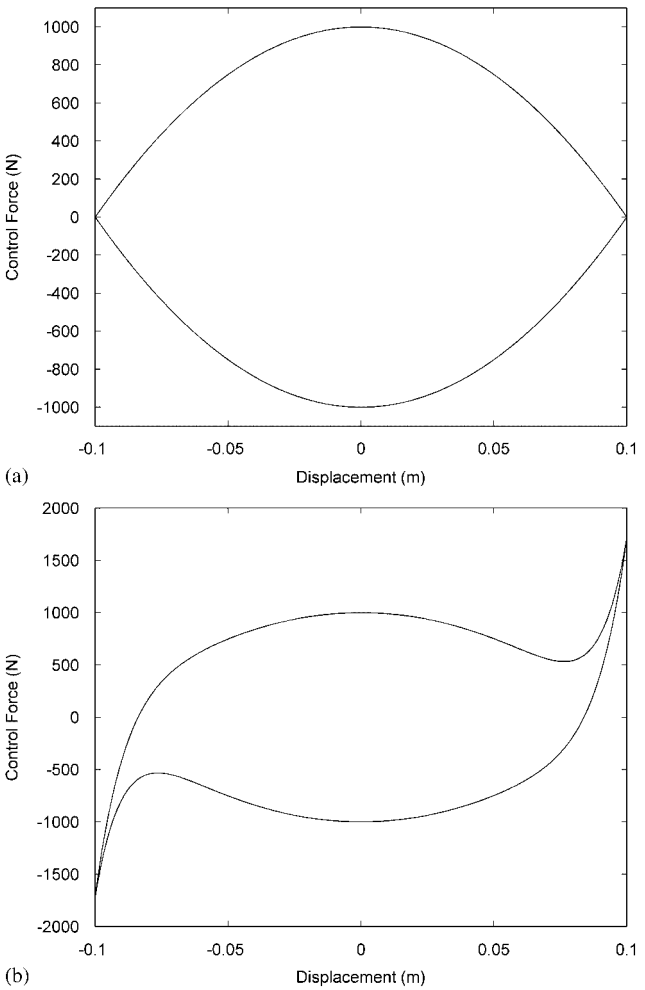


Figure 4. (a) Displacement force diagrams: standard viscous damper. (b) Displacement force diagrams: idealization of the cycle in Figure 3(b).



DOI: 10.1002/stc

which the first term in Equation (5) is modified in order to maintain the maximum value of the control force when the value of $a_v$ is varied.

Assuming the values of the parameters $k$ and $u_l$ as 600 N and 0.09 m, respectively, and applying a sinusoidal input function to the equation, the hysteresis loop shown in Figure 4(b) is obtained for $b = 1$ for the controller in Equation (5). It is observed that the resulting figure compares well with the previously obtained experimental loop between force and displacement drawn in Figure 3(b). The peak forces in Figures 3(b) and 4(b) differ by an order of magnitude. Actually, the experimental diagram of Figure 3(b) was obtained for a small prototype consistent with the limits of the available shaking table, while Figure 4(b) comes from the design of a device of performance comparable with that offered by the damper of capacity consistent with this benchmark study.

The parameter $k$ in Equation (5) is a global measure of the geometry (diameter and length) of the shape memory bars in the device, and it can be varied to achieve a desired force for any particular application. Likewise, parameter $u_l$ accounts for the contribution to the stiffness (symmetrically for positive and negative displacement). Peak displacement may be limited if $u_l$ is assumed to be very low. However, this may result in large values of shear and overturning moment. On the other hand, assuming a very large value of $u_l$ will make the damper response just governed by its nonlinear viscous damper part. Hence, the device parameters must be selected according to the expected peak bearing deformation. For an integrated design of the device with base isolator, the parameters of both the base isolator and the device can be optimized to achieve optimal performance in terms of peak response quantity reduction.

Note that all standard passive dampers have a limitation on the maximum stroke. The SMA device proposed in this paper incorporates those span limiters that should be coupled with the device during the construction and service lifetime so that a robust system is developed.

## RESPONSE ANALYSES

The SMA devices, represented by the analytical model in Equation (5), have been used as passive control devices, in order to improve the dynamic response of the bridge. Initially, for each ground acceleration record, four cases have been studied. Two values of $a_v$ have been selected as 0.6 and 2, corresponding to $b = 1$ and 7, respectively. Each of these values of $a_v$ has been paired with a low and a large value of $u_l$. These four cases described above are presented in Table II.

Table III presents a synthesis of the obtained results using all prescribed earthquake records. These results were obtained by adopting four different devices represented by cases from I to IV in Table II. In Table III, evaluation criteria showing improvement over those by sample passive case are marked in bold, whereas those performing worse are marked in italic. It can be observed from Table III that the evaluation criteria associated with the displacement decrease, but those associated with acceleration increase (i.e. a larger control force is required) when the value of the device parameter $u_l$ is decreased. Within Table III many benchmark indexes are not mentioned and attention is focused on the wished kinematics. Indeed the benchmark goal would be a decrease in the displacement indexes without a large increase in the acceleration indexes, being the latter ones related with the performance in terms of shear and overturning moment.

It is observed from Table II that the device in the case II for El Centro and N. Palm Springs earthquakes coincides with the device in case I for the other four earthquakes. It is noted from



DOI: 10.1002/stc

Table II. Synthesis of the four studied cases for the different records.

| | $a_v = 0.6$, $b = 1$ | | $a_v = 2$, $b = 7$ | |
|---|---|---|---|---|
| Record | Case I | Case II | Case III | Case IV |
| El Centro | $u_l = 0.065$ | $u_l = 0.090$ | $u_l = 0.060$ | $u_l = 0.090$ |
| N. P. Springs | $u_l = 0.065$ | $u_l = 0.090$ | $u_l = 0.060$ | $u_l = 0.090$ |
| Kobe | $u_l = 0.090$ | $u_l = 0.144$ | $u_l = 0.090$ | $u_l = 0.144$ |
| Turkey | $u_l = 0.090$ | $ul = 0.170$ | $ul = 0.090$ | $u_l = 0.170$ |
| Chichi | $u_l = 0.090$ | $u_l = 0.275$ | $u_l = 0.090$ | $u_l = 0.275$ |
| Rinadi | $u_l = 0.090$ | $u_l = 0.275$ | $u_l = 0.090$ | $u_l = 0.275$ |

Table III. Response due to all suggested ground records in the four studied cases: kinematics indexes.

| Performance index | Kobe | N. P. Springs | Chichi | El Centro | Northridge | Turkey |
|---|---|---|---|---|---|---|
| *Case I* | | | | | | |
| Peak displacement at mid-span | 0.468396 | 0.819546 | 0.421233 | 0.435718 | 0.451197 | 0.560103 |
| Peak acc at mid-span | *1.30537* | 1.17483 | *34.1454* | *1.70096* | *27.3346* | *8.25648* |
| Peak deformation of bearings | 0.46111 | 0.77129 | 0.337841 | 0.394791 | 0.338104 | 0.489897 |
| Normed displacement at mid-span | 0.660416 | *1.03678* | 0.596935 | 0.497832 | 0.604484 | 0.287327 |
| Normed acc at mid-span | *1.02874* | 0.913789 | *10.9331* | *1.21998* | *6.65822* | *2.13007* |
| Normed deformation of bearing | 0.68948 | 1.05606 | 0.61706 | 0.496314 | 0.573009 | 0.299864 |
| *Case II* | | | | | | |
| Peak displacement at mid-span | 0.710706 | 0.861185 | *0.83048* | 0.49036 | 0.849434 | 0.591009 |
| Peak acc at mid-span | *1.24506* | 1.17435 | *3.78284* | 1.05611 | *3.9709* | *0.926325* |
| Peak deformation of bearings | 0.69248 | 0.876666 | *0.806578* | 0.46838 | 0.828979 | 0.559591 |
| Normed displacement at mid-span | 0.873067 | 1.018 | 0.582212 | *0.47498* | 1.07772 | 0.499062 |
| Normed acc at mid-span | 0.991863 | 0.912704 | *1.52472* | *0.982077* | *1.69213* | 0.872944 |
| Normed deformation of bearing | 0.882924 | 1.02804 | 0.572609 | 0.494404 | *1.09722* | 0.499126 |
| *Case III* | | | | | | |
| Peak displacement at mid-span | 0.488588 | 0.721151 | 0.40102 | 0.421195 | 0.431546 | 0.518916 |
| Peak acc at mid-span | *1.86869* | 1.0515 | *20.4435* | *2.10337* | *21.1209* | *1.82896* |
| Peak deformation of bearings | 0.469206 | 0.707654 | 0.314778 | 0.367772 | 0.325644 | 0.444627 |
| Normed displacement at mid-span | 0.596263 | 1.00793 | 0.607115 | 0.274741 | 0.584359 | 0.255653 |
| Normed acc at mid-span | *1.10091* | *0.942523* | *7.13172* | *1.18817* | *5.24999* | *1.20622* |
| Normed deformation of bearing | 0.612916 | 1.01524 | 0.611295 | 0.261204 | 0.559141 | 0.252383 |
| *Case IV* | | | | | | |
| Peak displacement at mid-span | 0.74228 | 0.765993 | 0.65876 | *0.510682* | 0.725598 | 0.544266 |
| Peak acc at mid-span | *1.59293* | 1.05137 | 2.14913 | 1.05275 | *2.34717* | *1.15908* |
| Peak deformation of bearings | 0.722167 | 0.788064 | 0.653677 | 0.504031 | 0.714108 | 0.519669 |
| Normed displacement at mid-span | 0.966043 | 0.982434 | 0.594898 | *0.67825* | *0.792461* | 0.349601 |
| Normed acc at mid-span | *1.03056* | *0.943965* | *1.81028* | *1.02754* | *1.40227* | *0.955905* |
| Normed deformation of bearing | 0.98893 | 0.986587 | 0.602499 | *0.723513* | *0.792431* | 0.3478 |

Table III that this passive device, which can be regarded as satisfactory for the first two seismic events, becomes too weak for the other four events. The same remark applies to the devices in case IV for El Centro and N. Palm Springs earthquakes and the device in case III for other records.

The values of the evaluation criteria in Table IV are based on the best value of $u_l$ for each ground acceleration record, with $a_v$ and $b$ assigned to be 2 and 7, respectively, in all the cases, except for the Rinaldi earthquake, where $b$ is increased up to 5. The values of $u_l$ for each of the



DOI: 10.1002/stc

Table IV. Performance indexes for the sample passive device and the passive shape memory device (PSMD) under the different records.

| | Chichi | | Turkey | | Rinaldi | | Kobe | | El Centro | | N.P. | |
|---|---|---|---|---|---|---|---|---|---|---|---|---|
| Performance index* | Sample | PSMD | Sample | PSMD | Sample | PSMD | Sample | PSMD | Sample | PSMD | Sample | PSMD |
| *J*1:Peak base shear force | 0.91 | 0.88 | 0.78 | 1.19 | 1.07 | 1.37 | 0.91 | 1.06 | 0.62 | 1.41 | 1.06 | 1.21 |
| *J*2:Peak overturning moment | 0.95 | 1.07 | 0.70 | 1.28 | 1.04 | 1.37 | 0.90 | 1.15 | 0.61 | 1.37 | 1.10 | 1.37 |
| *J*3:Peak displacement at mid-span | *0.76* | *0.81* | 0.59 | 0.53 | 0.90 | 0.78 | 0.83 | 0.49 | 0.50 | 0.42 | 0.87 | 0.67 |
| *J*4:Peak acc. at mid-span | *1.13* | *2.39* | *0.92* | *1.29* | *1.05* | *1.90* | *1.16* | *1.87* | *1.09* | *2.10* | *1.17* | *1.62* |
| *J*5:Peak deformation of bearings | *0.76* | *0.80* | 0.56 | 0.48 | 0.90 | 0.77 | 0.83 | 0.47 | 0.49 | 0.37 | 0.88 | 0.62 |
| *J*6:Peak ductility | 0.95 | 1.07 | 0.70 | 1.28 | 1.04 | 1.37 | 0.90 | 1.15 | 0.61 | 1.37 | 1.10 | 1.37 |
| *J*9:Normed base shear force | 0.98 | 0.86 | 0.58 | 0.37 | 0.84 | 0.99 | 0.97 | 1.04 | 0.61 | 0.75 | 1.19 | 1.30 |
| *J*10:Normed overturning moment | 0.98 | 0.86 | 0.58 | 0.37 | 0.82 | 0.97 | 0.96 | 1.03 | 0.60 | 0.74 | 1.21 | 1.33 |
| *J*11:Normed displacement at mid-span | 0.98 | 0.86 | 0.52 | 0.22 | *0.76* | *0.78* | 0.96 | 0.60 | 0.59 | 0.27 | 1.02 | 0.82 |
| *J*12:Normed acc. at mid-span | *1.19* | *1.35* | *0.87* | *1.05* | *0.98* | *1.22* | *0.99* | *1.10* | *0.95* | *1.19* | *0.91* | *1.28* |
| *J*13:Normed deformation of bearing | 0.98 | 0.86 | 0.52 | 0.21 | *0.76* | *0.78* | 0.96 | 0.61 | 0.62 | 0.26 | 1.03 | 0.84 |
| *J*14:Normed ductility | 0.98 | 0.86 | 0.58 | 0.37 | 0.82 | 0.97 | 0.96 | 1.03 | 0.60 | 0.74 | 1.21 | 1.33 |
| *J*15:Peak control force | 0.00 | 0.02 | 0.00 | 0.02 | 0.00 | 0.02 | 0.00 | 0.02 | 0.00 | 0.02 | 0.00 | 0.01 |
| *J*16:Peak stroke in the control device | 0.76 | 0.80 | 0.56 | 0.48 | 0.90 | 0.77 | 0.83 | 0.47 | 0.49 | 0.37 | 0.88 | 0.62 |
| *J*19:No. of control devices | 20 | 20 | 20 | 20 | 20 | 20 | 20 | 20 | 20 | 20 | 20 | 20 |

*All other indexes introduced by the benchmark builders are calculated equal to zero.



DOI: 10.1002/stc

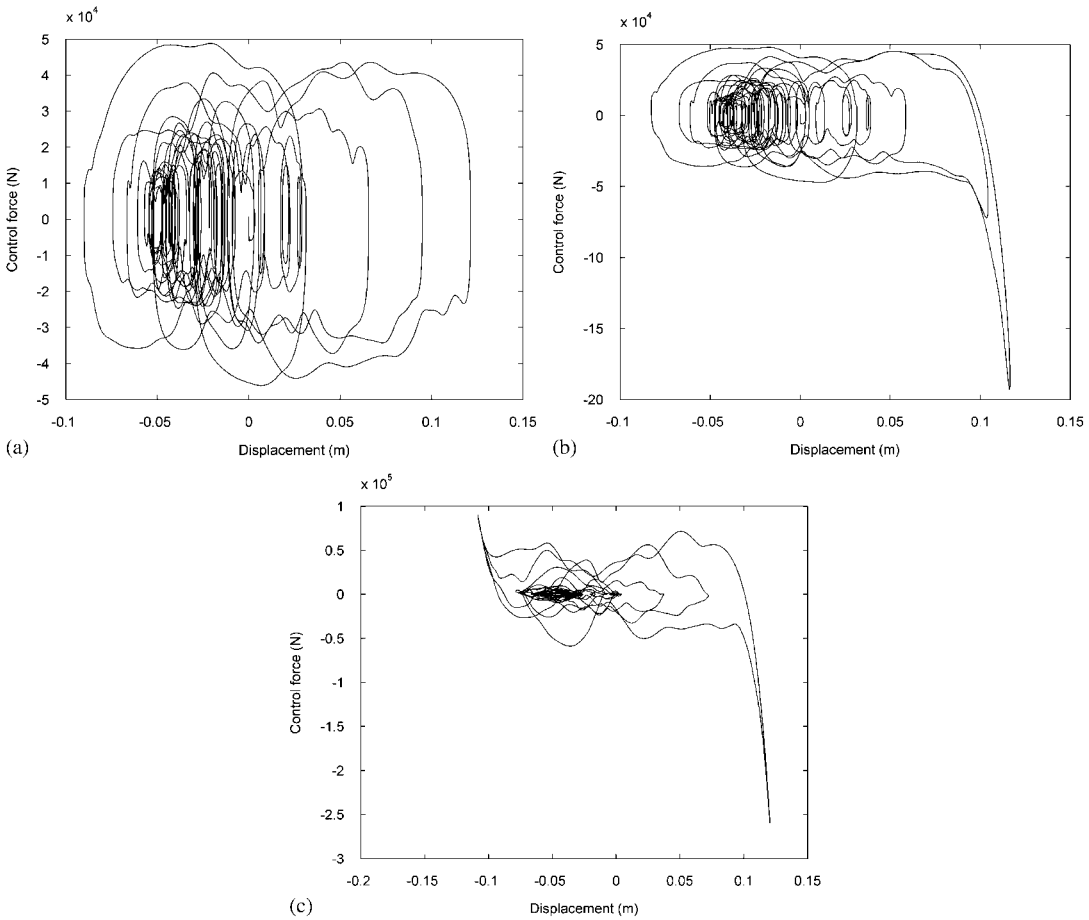


Figure 5. Force displacement loops in the device 19 (along the deck longitudinal direction) when the exciting ground acceleration record is the one labelled as El Centro: (a) original passive device; (b) proposed passive device (case II). (c) proposed passive device (case IV).

earthquake records are as follows: 0.29 m for Chichi, 0.105 m for Turkey, 0.31 m for Rinaldi, 0.09 m for Kobe, 0.06 m for El Centro and 0.045 m for North Palm Springs earthquakes.

Table IV also shows comparisons between the performance of the sample passive damper (denoted as 'Sample') and the proposed passive SMA device (denoted as 'PSMD'). Evaluation criteria (only for displacement and acceleration) performing better than those by sample passive have been marked in bold, while those performing worse have been italicized. It is observed from Table IV that the peak acceleration at the mid-span increases drastically even for 38% reduction in the peak bearing deformation. Except for a decrease in peak displacement and peak bearing deformation, decrease in other response quantities is not guaranteed during different earthquakes. Increase in accelerations is mainly due to the stiffness force contribution associated with the second addendum in the right hand side of Equation (5). Nevertheless, the proposed PSMD demonstrates the potential of designing effective damping systems that can aggressively



DOI: 10.1002/stc

limit peak bearing and other displacement response quantities during strong earthquakes at the cost of maximum 20% increase in peak base shear and a minimum 37% increase in overturning moment. Increase in these quantities can be reduced by the integrated design of the device and the PSMD.

Figure 5 shows the force displacement loop (hysteretic loop) of one of the devices in the longitudinal direction during El Centro ground motion. It is observed that the hysteretic loop modifies its shape with increase in displacement demand of the structure to aggressively limit peak dynamic response quantities, without demanding a semiactive policy [19].

## CONCLUSIONS

In this paper, we have presented applications of a passive shape memory alloy device (PSMAD) to the seismically excited highway bridge benchmark problem developed within the Matlab environment [20]. The behavior of this device can be modeled by coupling the elliptic, hysteretic force–displacement relationship of usual viscous devices with a nonlinear S-shape spring. The nonlinear viscous damper components dissipate input seismic energy, while the S-shape spring component limits peak dynamic response. The paper presents a detailed comparison of the simulation results for the PSMAD with those of passive sample controller. Simulation results show that while the PSMAD can reduce peak displacements, other response quantities such as peak base shear, peak overturning moment, peak mid-span acceleration, increase significantly. Nevertheless, the proposed approach can lead to an optimized passive solution that can protect the integrity of the bridge if both isolator and the PSMAD are designed in an integrated manner.

## ACKNOWLEDGEMENTS

A grant from the Athenaeum Research Fund of the University of Pavia did support the computational activity related with the results reported in this paper.

## REFERENCES

1. Spencer Jr BF, Dyke SJ, Deoskar HS. Benchmark problems in structural control: Part I—active mass driver system. *Earthquake Engineering and Structural Dynamics* 1998; **27**:1127–1140.
2. Spencer Jr BF, Dyke SJ, Deoskar HS. Benchmark problems in structural control—Part II: active tendon system. *Earthquake Engineering and Structural Dynamics* 1998; **27**(11):1141–1147.
3. Battaini M, Casciati F, Faravelli L. Fuzzy control of structural vibration. An active mass system driven by a fuzzy controller. *Earthquake Engineering and Structural Dynamics* 1998; **27**:1267–1276.
4. Yang JN, Agrawal AK, Samali B, Wu J-C. Benchmark problem for response control of wind-excited tall buildings. *Journal of Engineering Mechanics* (ASCE) 2004; **130**:437–446.
5. Battaini M, Casciati F, Faravelli L. Controlling wind response through a fuzzy controller. *Journal of Engineering Mechanics* (ASCE) 2004; **130**:486–491.
6. Erkus B, Johnson EA. Benchmark base isolated building with controlled bilinear isolation. *The 16th ASCE Engineering Mechanics Conference*, University of Washington, Seattle, 16–18 July 2003.
7. Nagarajaiah S, Narasimhan S. Smart base-isolated benchmark building. Part II: Phase I sample controllers for linear isolation systems. *Structural Control and Health Monitoring* 2006; **13**(2–3):589–604.
8. Narasimhan S, Nagarajaiah S, Gavin H, Johnson EA. Smart base-isolated benchmark building. Part I: Problem definition. *Structural Control and Health Monitoring* 2006; **13**(2–3):573–588.



DOI: 10.1002/stc

9. Narasimhan S, Nagarajaiah S, Johnson E. Structural control benchmark problem: Phase II—nonlinear smart base-isolated building subjected to near-fault earthquakes. *Structural Health Monitoring and Control* 2008; **15**(5):653–656.
10. Dyke SJ, Caicedo JM, Turan G, Bergman LA, Hague, S. Phase 1: benchmark control problem for seismic response of cable-stayed bridges. *Journal of Structural Engineering* (ASCE) 2003; **129**(7):857–872.
11. Caicedo JM, Dyke SJ, Moon SJ, Bergman LA, Turan G, Hague S. Phase II: benchmark control problem for seismic response of cable stayed bridges. *Journal of Structural Control* 2003; **10**:137–168.
12. Bontempi F, Casciati F, Giudici M. Seismic response of a cable-stayed bridge: active and passive control systems (benchmark problem). *Journal of Structural Control* 2003; **10**:169–185.
13. Agrawal A, Tan P, Nagarajaiah S, Zhang J. Benchmark structural control problem for a seismically excited highway bridge—Part I: Phase I problem definition. *Journal of Structural Control and Health Monitoring*, 2008. DOI: 10.1002/stc.301.
14. Tan P, Agrawal AK. Benchmark structural control problem for a seismically excited highway bridge—Part II: Phase I sample control design. *Journal of Structural Control and Health Monitoring* 2008. DOI: 10.1002/stc.300.
15. Nagarajaiah S, Narasimhan S, Agrawal A, Ping T. Benchmark structural control problem for a seismically excited highway bridge—Part III: Phase II sample controller for the fully base-isolated case. *Journal of Structural Control and Health Monitoring*, 2008. DOI: 10.1002/stc.293.
16. Casciati F, Faravelli L, Hamdaoui K. Performance of a base isolator with shape memory alloy bars. *Earthquake Engineering and Engineering Vibration* 2007; **6**(4):401–408.
17. Casciati F, Hamdaoui K. Modelling the uncertainty in the response of a base isolator. *Probabilistic Engineering Mechanics* 2008; **23**(4):427–437.
18. Casciati F, Faravelli L. A passive control device with SMA components from the prototype to the model. *Structural Control and Health Monitoring* 2008. DOI: 10.1002/stc.322.
19. Casciati F, Magonette G, Marazzi F. *Semi-active Devices and Applications in Vibration Mitigation*. Wiley: Chichester, UK, 2006.
20. MATLAB, The Math Work, Inc., 2004.